JCTC Journal of Chemical Theory and Computation

Bonding in Low-Coordinate Environments: Electronic Structure of Distorted Square-Planar Iron-Imido Complexes With Pincer-Type Ligands

Jeanet Conradie[†,‡] and Abhik Ghosh*[,†]

Department of Chemistry and Center for Theoretical and Computational Chemistry, University of Tromsø, N-9037 Tromsø, Norway, and Department of Chemistry, University of the Free State, 9300 Bloemfontein, Republic of South Africa

Received April 6, 2008

Abstract: Low-coordinate architectures sustain unusual chemistry for middle and late transition metals, of which imido complexes are an excellent example. Recent DFT studies have uncovered a number of unusual features in the bonding in trigonal-planar and pseudotetrahedral imido complexes. Herein, we have extended these studies to a unique, distorted square-planar iron-imido complex with a pincer-type pyridine-2,6-diimine (PDI) supporting ligand. DFT calculations indicate that the iron center in the formally Fe(II) complex Fe(PDI)(NPh) is better described as intermediate-spin Fe(III), antiferromagnetically coupled to a b_2-symmetry PDI π-anion radical. A comparative analysis of the major classes of low-coordinate imido complexes has uncovered a certain similarity between Fe(PDI)(NPh) and a trigonal-planar Fe(III)-nacnac-imido complex. Both ligand architectures afford a total of four energetically accessible d orbitals, resulting in intermediate-spin Fe(III) centers.

Introduction

Middle and late transition metal-imido complexes have remained rather elusive until quite recently. Undoubtedly, the strong metal(d_π)-N_{imido}(p_π) antibonding interactions that many such complexes would entail have stood in the way of their synthesis and characterization. The use of low-coordinate architectures, however, has recently led to the synthesis of a number of trigonal-planar and pseudotetrahedral iron-,[1,2] cobalt-,[3,4] and nickel-[5] imido complexes. The bonding in these complexes has unusual features, which we have analyzed with density functional theory calculations in the course of a number of papers.[6−8] One middle transition metal-imido complex that has so far escaped a quantum chemical analysis is an iron-imido complex with a pincer-type pyridine-2,6-diimine (PDI) supporting ligand.[9] We undertook a theoretical study of this complex, not only on account of its distorted square-planar geometry, which is unique for an iron-imido complex, but also to examine the proposal that this formally Fe^{II}-imido species is better described as an Fe^{III}-imido $PDI^{\bullet-}$ radical.[9] Our goal, first and foremost, was to arrive at a qualitative molecular orbital description for this complex. Accordingly, we adopted a spin-unrestricted (broken-symmetry) density functional theory (DFT) approach in this study, even though some might have preferred considerably more demanding multiconfigurational *ab initio* methods (such as the popular CASPT2 method) for this problem.[10,11] DFT has been extensively and successfully applied to a variety of noninnocent[12,13] ligands (and metalloradicals), and we will see that our calculations nicely confirm the Fe(III) PDI-anion-radical description proposed by the experimentalists.

Methods

In general, all calculations used the OLYP[14,15] generalized gradient approximation (GGA), triple-ζ plus polarization Slater-type orbital basis sets, and a fine mesh for numerical integration of the matrix elements, all as implemented in the ADF2006 program system.[16] The choice of OLYP as the default functional is based on a number of recent studies from our laboratory, where OLYP proved to be one of the

* Corresponding author e-mail: abhik@chem.uit.no.
† University of Tromsø.
‡ University of the Free State.

10.1021/ct800118c CCC: $40.75
Published on Web 09/13/2008

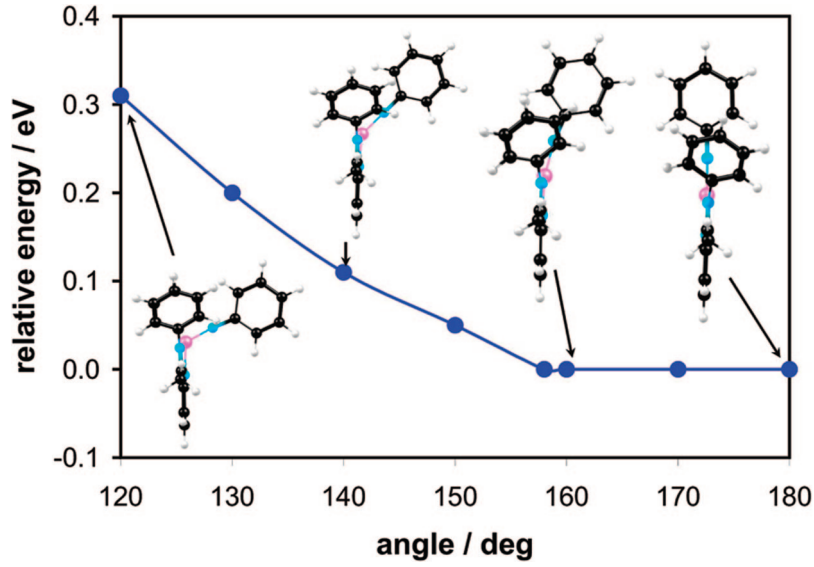

Figure 1. Potential energy of Fe(PDI)(NPh) as a function of out-of-plane bending of the Fe−N−C_{Ph} angle.

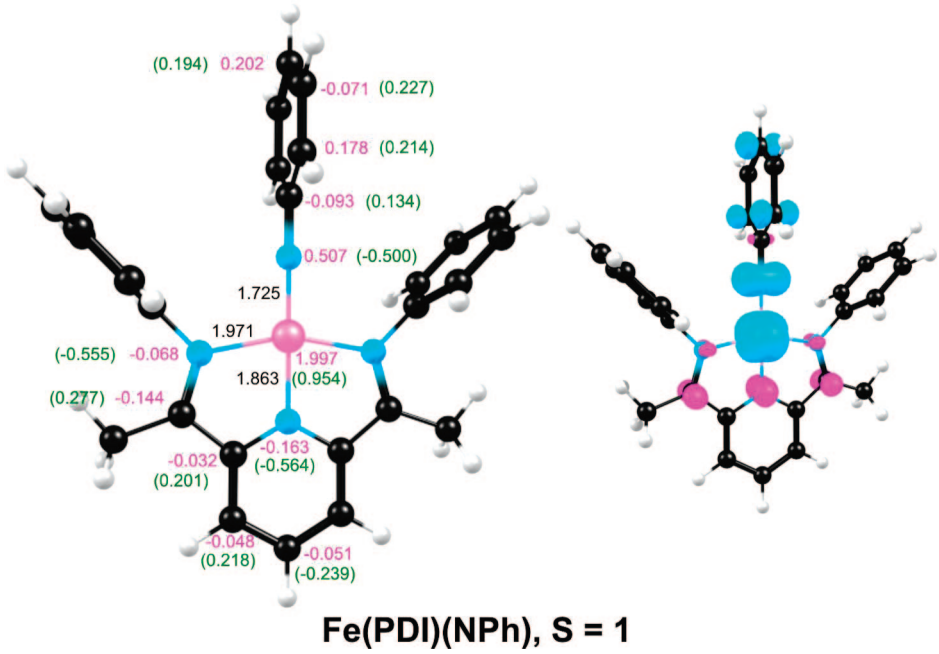

Figure 2. Ground-state ($M_S = 1$) OLYP/TZP results of Fe(PDI)(NPh) (C_{2v}). The diagrams to the left depict bond distances (Å, in black), Mulliken spin populations (magenta), and charges (green). Spin density plots are shown to the right (majority spin in cyan, minority spin in magenta). Color code for atoms: C (black), H (ivory), N (cyan), and Fe (pink).

better functionals for transition metal systems.[6−8] Most calculations were also repeated with other functionals, including PW91,[17] BP86,[18] BLYP,[19,15] PBE,[20] B3LYP,[21,15] and B3LYP*.[22,15]

The experimentally characterized iron-imido complex that we sought to model is based on the $^{i\mathrm{Pr}}$PDI (= 2,6-^{i}Pr$_2$C$_6$H$_3$-N=CMe)$_2$C$_5$H$_3$N) ligand.[9] In our calculations, we chose a simpler version of the ligand, viz. PDI (=PhN=CMe)$_2$-C$_5$H$_3$N). In the same spirit, we chose the simple phenylimido ligand as the fourth ligand, whereas a more sterically hindered arylimido ligand was employed experimentally. Although the experimentally studied complex exhibits a bent Fe−N_{imido}−C_{Ar} angle, our calculations showed that deformation of this angle is exceedingly soft, as shown in Figure 1. Much of our analysis of the Fe(PDI)(NPh) model complex is therefore based on a C_{2v} geometry. In general, we found that the NPh group prefers to orient itself perpendicular to the plane of the pyridine group.

Finally, to better appreciate the neutral Fe(PDI)(NPh) complex, we have also studied the low-lying electronic states of the $[Fe(PDI)(NPh)]^+$ cation.

Results

(a). Basic Electronic-Structural Description of Ground-State Fe(PDI)(NPh). Figure 2 depicts selected OLYP/TZP results for Fe(PDI)(NPh), optimized under a C_{2v} symmetry constraint. The bond distances to iron in the S = 1 optimized

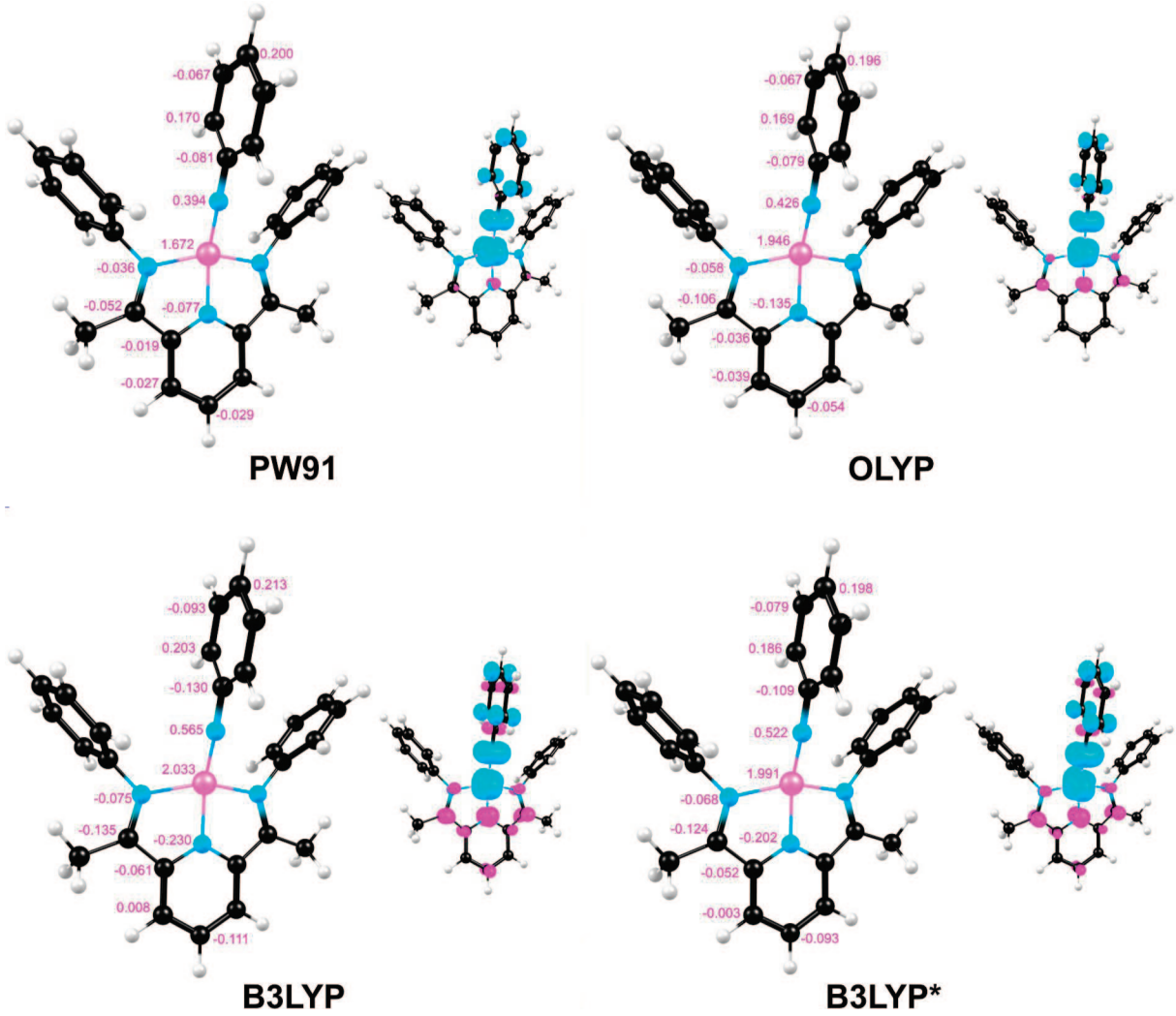

Figure 3. Mulliken spin populations and spin density plots (majority spin in cyan, minority spin in magenta) for the S = 1 ground-state of Fe(PDI)(NPh) for different functionals. Color code for atoms: same as in Figure 2.

structure of Fe(PDI)(NPh) (Figure 2) agree quite well with experiment:[9] Fe−N_{imido} 1.725 Å (expt. avg. 1.711 Å), Fe−$N_{pyridine}$ 1.863 Å (expt. avg. 1.856 Å), and Fe−N_{imino} 1.971 Å (expt. avg. 2.0224 Å). A major difference between the optimized C_{2v} structure and that observed experimentally is that the imido linkage in the latter is strongly bent out of the PDI plane. However, as mentioned above, a potential energy curve as a function of out-of-plane Fe−N_{imido}−C bending (under a C_s symmetry constraint) revealed an exceedingly flat potential; hence the use of a C_{2v} constraint appeared both convenient and justifiable.

The ground-state OLYP spin density profile of Fe(PDI)(NPh) shown in Figure 2 is of considerable interest. The majority spin density, largely localized on the Fe═NPh moiety, adds up to about 3 electrons; the minority spin density is localized largely on the PDI ligand and adds up to about 1 electron. In other words, the PDI ligand appears to be noninnocent, and the complex, overall, appears to be describable as an S = 3/2 Fe(III) $PDI^{\bullet-}$ anion radical. (Of course, broken-symmetry solutions such as this one do not correspond to a specific spin state or S but rather only to $M_S = 1$. However, the solution is *predominantly* S = 1, and, accordingly, the spin density profile indicated in Figure 2 is certainly a qualitative approximation to the true triplet spin density.) Figure 3 depicts the same (i.e., $M_S = 1$) spin density profile, obtained with three additional functionals. Observe that the classic pure functional PW91 provides a more covalent spin density relative to OLYP; i.e. there is less spatial separation of majority and minority spin density with PW91. The hybrid functional B3LYP behaves oppositely, producing the largest separation of majority and minority spin densities. In contrast, B3LYP*, which has a reduced amount of Hartree−Fock exchange (15%) relative to B3LYP (20%), yields a more or less OLYP-like spin density profile. The $\langle S^2 \rangle$ value (ideally 2.0) obtained with the different functionals may be correlated with these findings: PW91 2.137, OLYP 2.345, B3LYP* 2.534, and B3LYP 2.655.

To place the above results in context, we also carried out OLYP/TZP calculations on Fe(PDI)(O) and Fe(PDI)Cl_2; highlights of the results are shown in Figure 4. Not surprisingly, the spin density profile of the S = 1 ferryl species is rather similar to that described above for Fe(PDI)(NPh), implicating a similar S = 3/2 Fe(III) $PDI^{\bullet-}$ electronic description. In contrast, Fe(PDI)Cl_2 exhibits an S = 2 high-spin Fe(II) ground state, as found for a similar

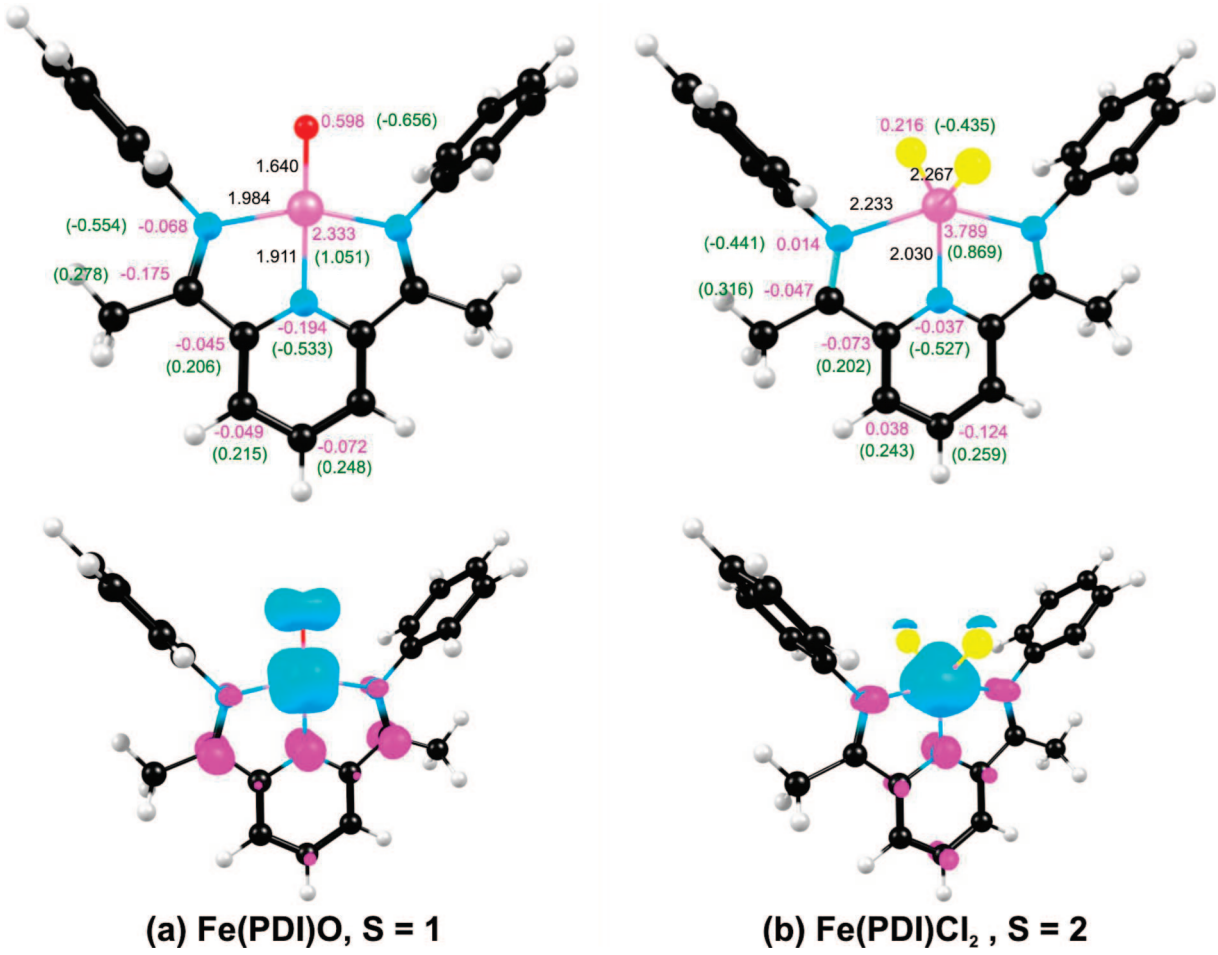

Figure 4. OLYP/TZP results for the lowest-energy states of Fe(PDI)(O) (C_{2v}) and Fe(PDI)Cl_2 (C_{2v}). The diagrams at the top depict bond distances (Å, in black), Mulliken spin populations (magenta), and charges (green). Spin density plots are shown in the lower row (majority spin in cyan, minority spin in magenta). Color code for atoms: same as in Figure 2, O (red) and Cl (yellow).

complex in the literature, although it too exhibits small amounts of minority spin density based on the PDI.[23]

An examination of the Kohn−Sham orbitals of Fe(PDI)(NPh), as shown in Figure 5, now allows a more detailed description of its electronic configuration. Aligning the Fe-NPh vector along the z axis and the mean plane of the PDI ligand along the xz plane, we may describe the symmetries of the five d orbitals as follows:

a_1 : $d_{y_2}(a_{1\text{-}2})$, $d_{x2\text{-}z2}(a_{1\text{-}1})$

a_2: d_{xy}

b_1: d_{xz}(also describable as π_{xz}*)

b_2: d_{yz}(also describable as π_{yz}*)

The electronic configuration of the iron center may now be described as $(d_{xy})^2(d_{y2})^1(\pi_{xz}^*)^1(\pi_{yz}^*)^1$. However, an examination of the b_2 minority-spin HOMO, which has some d_{yz} character, indicates that it is primarily a PDI-based MO. Thus, the MO energy level diagram shown in Figure 5 provides a rather straightforward confirmation of the S = 3/2 Fe(III) $PDI^{\bullet-}$ electronic description alluded to above. Simple group-theoretic arguments now indicate that the electronic ground state of Fe(PDI)(NPh) is $^3B_1$, where the b_1 irrep is symmetric with respect to reflection across the PDI plane.

(b) Spin-State Energetics. For DFT calculations on transition metal compounds, the question of relative energetics of different spin states is a significant one. Exploiting C_{2v} symmetry of Fe(PDI)(NPh), we have been able to optimize a number of different occupations as well as cationic states. Table 1 lists the relative energetics of the various charge-neutral states of Fe(PDI)(NPh) for different functionals, while Figure 6 depicts selected geometry parameters, Mulliken charges, spin populations, and spin density plots.

All the functionals yield the same S = 1 ground state. An open-shell singlet low-spin $(d_{xy})^2(d_{y2})^2(\pi_{yz}^*)^1$ Fe(III) state with an antiferromagnetically coupled b_2 $PDI^{\bullet-}$ radical is over an eV higher in energy, regardless of the functional. In contrast, a closed-shell singlet $(d_{xy})^2(d_{y2})^2(\pi_{yz}^*)^2$ "Fe(II)" state is significantly lower in energy, about 0.3−0.6 eV for pure functionals and about 1 eV for hybrid functionals.

All the functionals also predict a fairly low-energy quintet state, at about half an eV above the ground state; this state is best described as intermediate-spin $(d_{xy})^2(d_{y2})^1(\pi_{xz}^*)^1$-$(\pi_{yz}^*)^1$ Fe(III) ferromagnetically coupled to a b_2 $PDI^{\bullet-}$ radical. With a spin population of 2.222 (as shown in Figure 6), the iron center is clearly not high-spin, i.e. not S = 5/2 Fe(III).

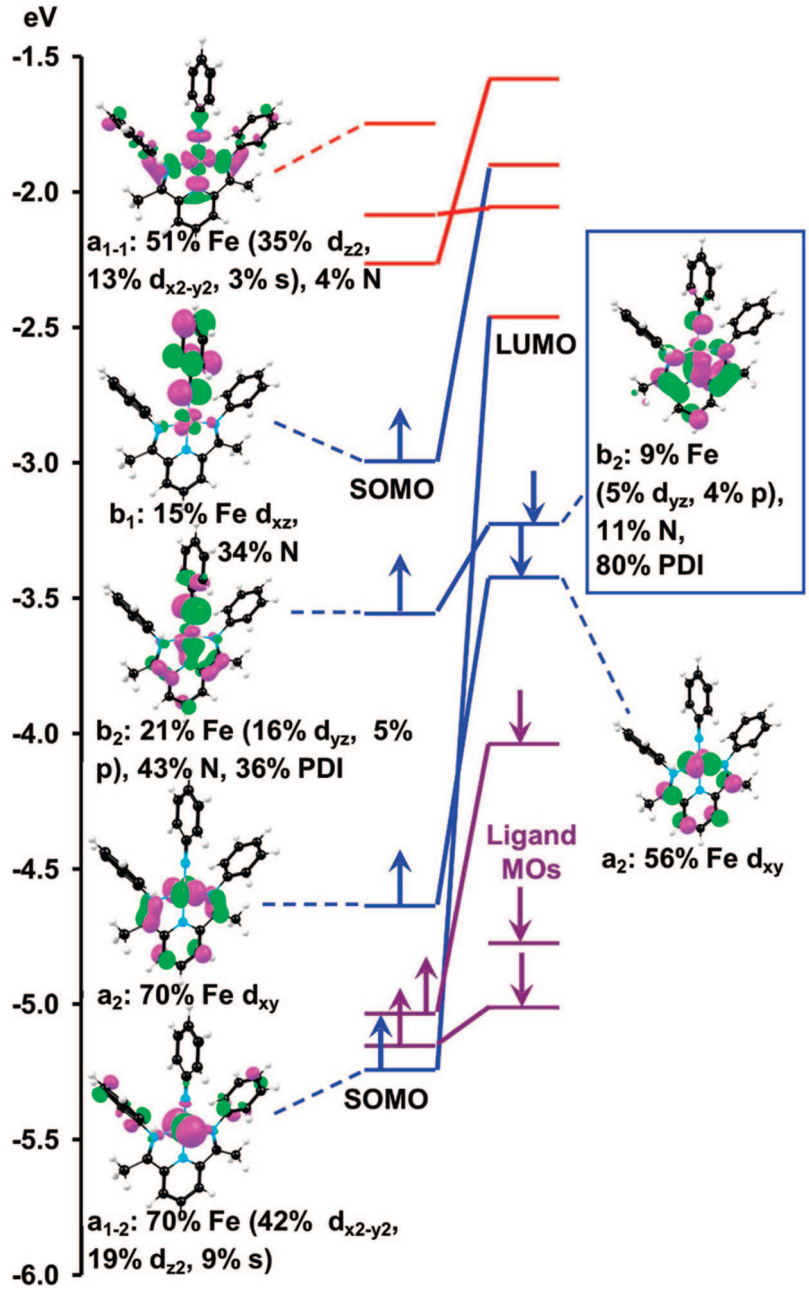

Figure 5. OLYP/TZP MO energy level diagram for the S = 1 ground state of Fe(PDI)(NPh). Note that whereas the α-spin b_2 HOMO has 64% Fe=NPh character and only 36% PDI character, a reverse situation applies for the β-spin b_2 HOMO (shown in the blue box), which is overwhelmingly (80%) PDI-based. Metal d-based occupied MOs are indicated in blue, occupied ligand-based MOs in maroon, and unoccupied MOs in red.

For the septet state, involving a high-spin Fe(III) center ferromagnetically coupled to a b_2 $PDI^{\bullet -}$ radical, the energy is strongly functional-dependent. Thus, whereas with pure functionals the energy hovers in the range 1.1 ± 0.3 eV, B3LYP predicts an energy of only 0.33 eV relative to the ground state. As elsewhere, B3LYP* (with a reduced amount of Hartree−Fock exchange, 15%, relative to B3LYP) yields an intermediate energy of about 0.6 eV.[24]

Recently, Chirik and co-workers have reported detailed spectroscopic and theoretical studies of reduced Fe(PDI) complexes, including many with neutral ligands. Theory and experiment concur that a number of these species contain $PDI^{\bullet\bullet 2-}$ dianion-diradical ligands.[23] However, such an electronic-structural description does not appear to be relevant for the species examined in this study.

(c) The $[Fe(PDI)(NPh)]^+$ Cation. We have briefly studied the $[Fe(PDI)(NPh)]^+$ cation with OLYP/TZP optimizations of the lowest S = 1/2, 3/2, and 5/2 states, in case it is generated and characterized in the future. Unfortunately, the calculations do not afford a reliable energy ordering of the three states. The doublet and the quartet are approximately equienergetic, whereas the sextet is several tenths of an electronvolt higher in energy. These relative energies could be easily upset with other functionals as well as with more accurate quantum chemical methods such as CASPT2. Figure 7 presents selected results for the $[Fe(PDI)(NPh)]^+$ cation.

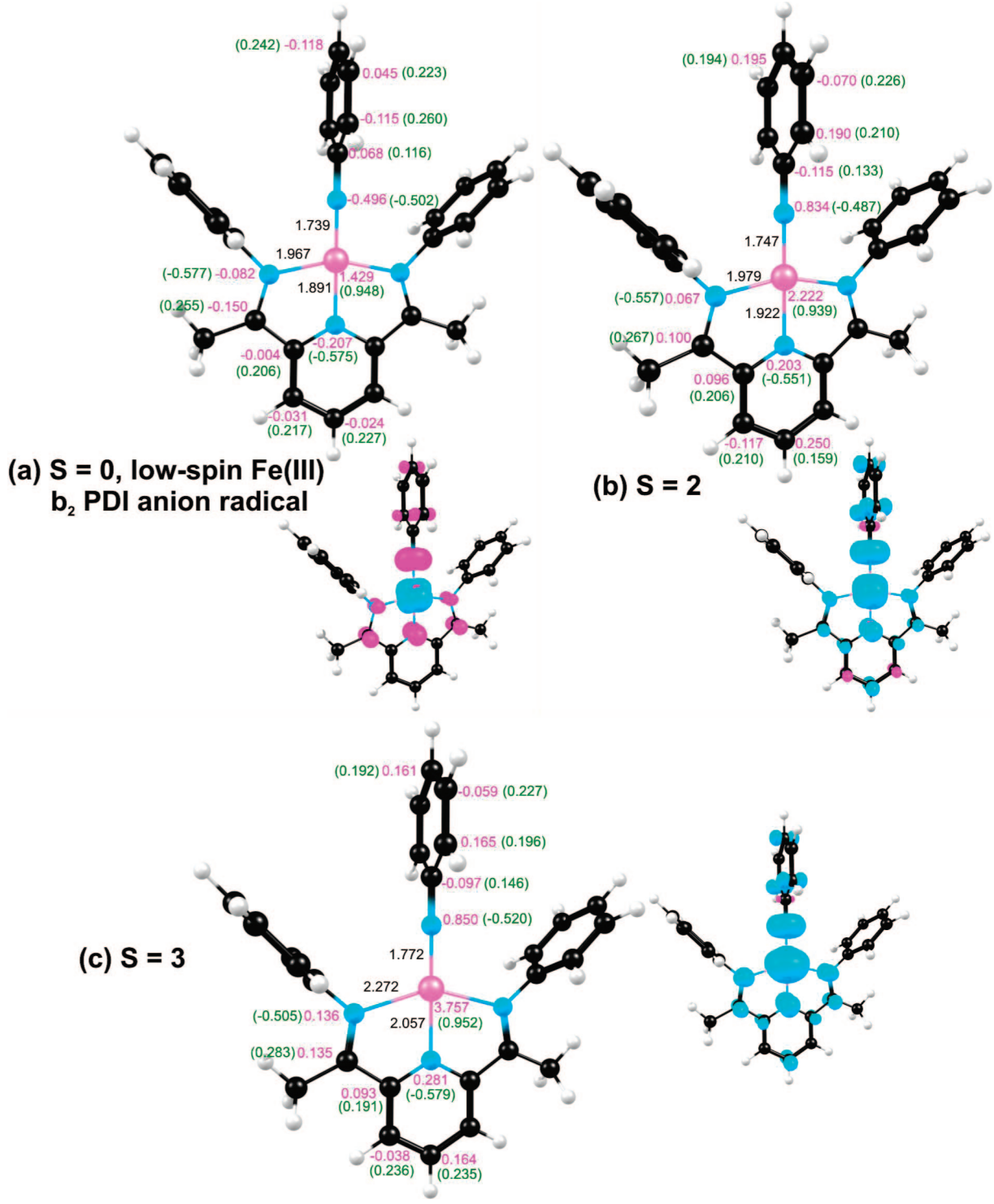

Figure 6. OLYP/TZP results for the selected excited states of Fe(PDI)(NPh), optimized under a C_{2v} symmetry constraint. The diagrams to the left depict bond distances (Å, in black), Mulliken spin populations (magenta), and charges (green). Spin density plots are shown to the right (majority spin in cyan, minority spin in magenta). Color code for atoms: same as in Figure 2.

The cationic S = 3/2 state is best described as an intermediate-spin Fe(III) state with a $(d_{xy})^2(d_{y2})^1(\pi_{xz}^*)^1(\pi_{yz}^*)^1$ configuration, just like the ground-state neutral species (see above). (In other words, the b_2 π-radical electron has been lost.) Occupancy of both π^* orbitals results in a substantial spin density on the imido nitrogen, exactly as in the case of the ground-state neutral. In contrast, the cationic S = 1/2 state is best described as a $(d_{xy})^2(d_{y2})^1(\pi_{yz}^*)^1$ Fe(IV) center antiferromagnetically coupled to a b_2 $PDI^{\bullet-}$ anion radical. The low energy of this state once again demonstrates the strong tendency of the Fe-imido unit to adopt a higher oxidation state and that of the PDI ligand to become an anion radical.

Discussion

Armed with a basic description of the electronic structure of the complex of interest in this study, we can now attempt

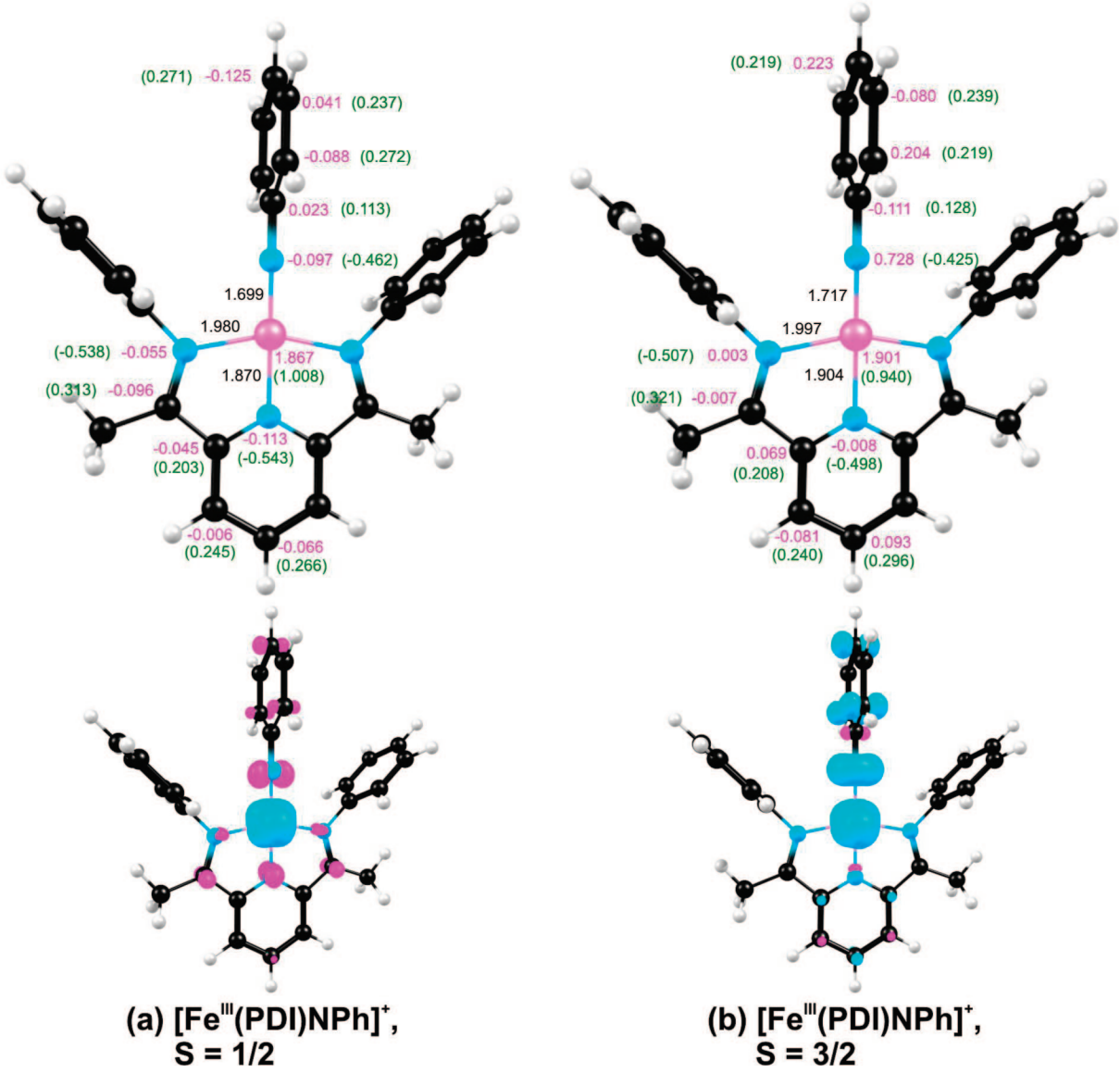

Figure 7. OLYP/TZP results for the lowest-energy S = 1/2 and 3/2 states of [Fe(PDI)(NPh)]$^+$ (C_{2v}). The diagrams at the top depict bond distances (Å, in black), Mulliken spin populations (magenta), and charges (green). Spin density plots are shown below (majority spin in cyan, minority spin in magenta). Color code for atoms: same as in Figure 2.

to contextualize it vis-à-vis recent findings on low-coordinate middle and late transition metal-imido complexes. The optimized Fe−N_{imido} distance of 1.725 Å is similar to that we calculated for a three-coordinate Fe^{III}(nacnac)(NPh) model complex[7] (the Fe−N_{imido} distances for the relevant experimentally studied complexes are also similar). The similarity is not unexpected, given that both species feature intermediate-spin Fe^{III}-imido units, with a single Fe(d_π)−N_{imido}(p_π) antibonding interaction. In contrast, low-spin (S = 1/2) tris(phosphine)-supported Fe^{III}-imido complexes exhibit shorter Fe−N distances of about 1.65 Å, consistent with the lack of any Fe(d_π)−N_{imido}(p_π) antibonding interactions.[1,6]

A recurring theme in the low-coordinate imido literature seems to be that many of the complexes are low- or intermediate-spin, rather than high-spin.[1,6−8] In other words, the d electrons tend to avoid MOs with Fe(d_π)−N_{imido}(p_π) antibonding interactions.[25] One feature of many low-coordinate complexes that helps in this is that typically there is no ligand *trans* to the imido ligand, which results in a dramatic lowering of the energy of the d_{z2}-like orbital, i.e. the d_σ orbital pointing directly at the imido group. Thus, despite its formal σ-antibonding designation, this orbital often provides a remarkably low-energy "home" for one or two electrons, which would otherwise be forced to occupy high-energy π^* MOs.

Clearly, the above bonding paradigm does not hold for Fe(PDI)(NPh). As shown in Figure 5 and re-emphasized in Figure 8, the Fe d_σ-based orbital that points directly toward the imido group−the d_{x2-z2}-based a_{1-1} MO−is not a low-energy orbital but a high-energy, unoccupied MO. As may be seen from Figure 5, this is the orbital in a typical square-planar complex that is destabilized by four relatively head-on σ-antibonding interactions involving the four ligands. Note from Figure 8, however, that except for this one orbital, the d orbital ordering in Fe(PDI)(NPh)

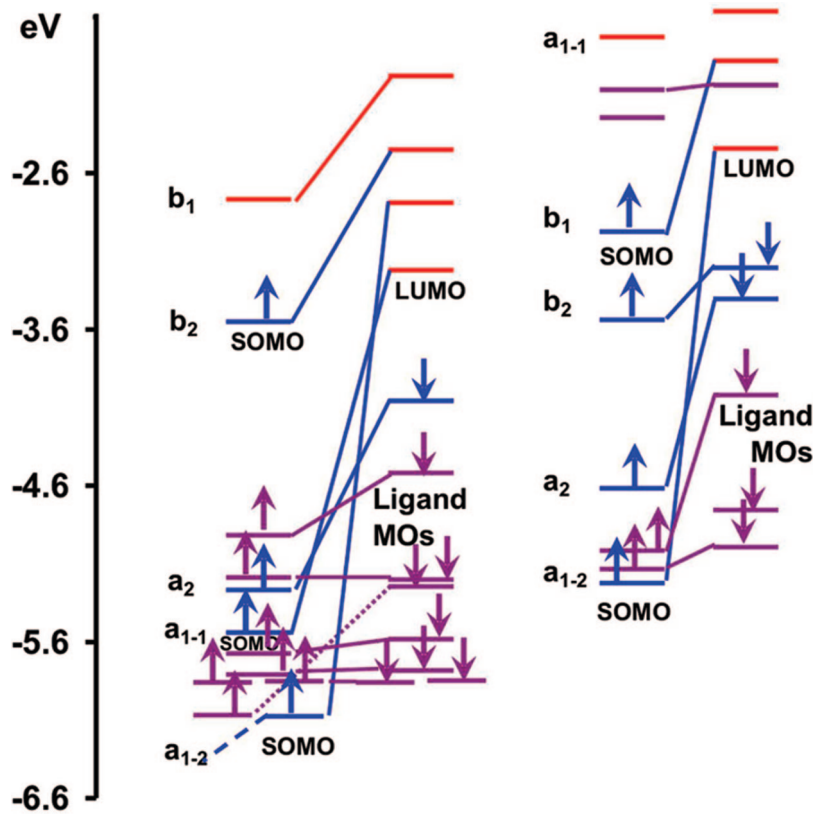

Figure 8. A comparison of the OLYP Kohn−Sham metal d-based MO energy levels of Fe(PDI)(NPh) (C_{2v}, S = 1, right) with Fe^{III}(nacnac)(NPh) (C_{2v}, S = 3/2, left). Metal d-based occupied MOs are indicated in blue, occupied ligand-based MOs in maroon, and unoccupied MOs in red.

Table 1. Relative Energies (eV) of Different Spin States of Fe(PDI)(NPh), Optimized under a C_{2v} Symmetry Constraint[a]

state	occupation	PW91	BP86	BLYP	OLYP	PBE	B3LYP	B3LYP*
S = 1	A1 51//50 A2 13//13 B1 34//33 B2 23//23	**0.00**	**0.00**	**0.00**	**0.00**	**0.00**	**0.00**	**0.00**
S = 0, open-shell	A1 51//50 A2 13//13 B1 33//33 B2 23//24	1.18	1.18	1.14	1.27	1.18	1.08	1.12
S = 0, spin-restricted	A1 51//51 A2 13//13 B1 33//33 B2 23//23	0.32	0.31	3.12	0.49	0.29	1.10	0.85
S = 2	A1 51//50 A2 13//13 B1 34//33 B2 24//22	0.72	0.69	0.67	0.61	0.69	0.46	0.52
S = 3	A1 52//50 A2 13//12 B1 34//33 B2 24//22	1.39	1.32	1.26	0.80	1.34	0.33	0.59

[a] The S = 1 state has been chosen as the energy zero level.

is identical to that in Fe^{III}(nacnac)(NPh),[2] a molecule whose metal d-based MOs are topologically quite similar to those of Fe(PDI)(NPh).[7]

Another key distinction between the MO energy levels of the two complexes involves the "in-plane" Fe(d_{xz})−N_{imido}(p_x) π-antibonding MO (b_1). In the case of trigonal-planar Fe^{III}(nacnac)(NPh), this MO is additionally destabilized by σ-antibonding interactions with the nacnac nitrogens and is therefore unoccupied. By contrast, no analogous σ-antibonding interaction with the PDI ligand is expected (or found) for either of the Fe−N_{imido} π* MOs of square-planar Fe(PDI)(NPh). Thus, both these π* MOs are singly occupied for Fe(PDI)(NPh), whereas only one such MO is (singly) occupied for Fe^{III}(nacnac)(NPh). This distinction translates into a significant difference vis-à-vis the spin density profiles of the two complexes: in

essence, the former exhibits a much higher N_{imido} spin population (0.51, see Figure 2) than the latter (0.13).[7]

Despite the above differences, there are intriguing similarities between the PDI and nacnac complexes. Both architectures result in a single energetically inaccessible d orbital, viz. the a_{1-1} orbital in the case of Fe(PDI)(NPh) and the (above-mentioned) b_1 orbital for the nacnac complex. Both complexes thus afford four energetically accessible d orbitals, resulting in intermediate-spin Fe(III) centers.

Conclusions

In conclusion, the iron center in the formally Fe(II) complex Fe(PDI)(NPh) is better described as intermediate-spin Fe(III), antiferromagnetically coupled to a b_2-symmetry PDI π-anion radical. With this study completed, we now have a basic theoretical survey of the major known classes of low-coordinate transition metal imido complexes. Intriguing similarities and differences have emerged between the orbital structure of Fe(PDI)(NPh) and that of a trigonal-planar Fe(III)-nacnac-imido complex. Despite key differences, both architectures, it turns out, afford a total of four energetically accessible d orbitals, thereby engendering intermediate-spin Fe(III) centers.

Acknowledgment. This work was supported by the Research Council of Norway (AG) and the National Research Fund of the Republic of South Africa (grant no. 61093).

Supporting Information Available: Table of optimized Cartesian coordinates. This material is available free of charge via the Internet at http://pubs.acs.org.

References

(1) For a review, see: Mehn, M. P.; Peters, J. C. *J. Inorg. Biochem.* **2006**, *100*, 634–643.

(2) Eckart, N. A.; Vaddadi, S.; Stoian, S.; Lachicotte, R. J.; Cundari, T. R.; Holland, P. L. *Angew. Chem., Int. Ed.* **2006**, *45*, 6868–6871.

(3) In addition to references cited in ref 1, see: Cowley, R. E.; Bontchev, R. P.; Sorrell, J.; Sarracino, O.; Feng, Y.; Wang, H.; Smith, J. M. *J. Am. Chem. Soc.* **2007**, *129*, 2424–2425.

(4) Dai, X.; Kapoor, P.; Warren, T. H. *J. Am. Chem. Soc.* **2004**, *126*, 4798–4799.

(5) Kogut, E.; Wiencko, H. L.; Zhang, L. B.; Cordeau, D. E.; Warren, T. H. *J. Am. Chem. Soc.* **2005**, *127*, 11248–11249.

(6) Tangen, E.; Conradie, J.; Ghosh, A. *J. Chem. Theory Comput.* **2007**, *3*, 448–457.

(7) Conradie, J.; Ghosh, A. *J. Chem. Theory Comput.* **2007**, *3*, 689–702.

(8) Wasbotten, I. H.; Ghosh, A. *Inorg. Chem.* **2007**, *46*, 7890–7898.

(9) Bart, S. C.; Lobkovsky, E.; Bill, E.; Chirik, P. J. *J. Am. Chem. Soc.* **2006**, *128*, 5302–5303.

(10) Aquilante, F.; Malmqvist, P.-Å.; Pedersen, T. B.; Ghosh, A.; Roos, B. O. *J. Chem. Theory Comput.* **2008**, *4*, 694–702.

(11) Ghosh, A.; Gonzalez, E.; Tangen, E.; Roos, B. O. *J. Phys. Chem. A***2008**; ASAP Article; DOI: 10.1021/jp711159h (http://pubs.acs.org/cgi-bin/abstract.cgi/jpcafh/asap/abs/jp711159h.html).

(12) For a review, see: Ghosh, A. *J. Biol. Inorg. Chem.* **2006**, *11*, 712–724.

(13) For another DFT study of noninnocent ligands, see:(a) Ghosh, P.; Bill, E.; Weyhermuller, T.; Neese, F.; Wieghardt, K. *J. Am. Chem. Soc.* **2003**, *125*, 1293–1308.

(14) The OPTX exchange functional: Handy, N. C.; Cohen, A. J. *Mol. Phys.* **2001**, *99*, 403–412.

(15) The LYP correlation functional: Lee, C.; Yang, W.; Parr, R. G. *Phys. Rev. B* **1988**, *37*, 785–789.

(16) The ADF program system was obtained from Scientific Computing and Modeling, Amsterdam (http://www.scm-.com/). For a description of the methods used in ADF, see: (a) Velde, G. T.; Bickelhaupt, F. M.; Baerends, E. J.; Guerra, C. F.; Van Gisbergen, S. J. A.; Snijders, J. G.; Ziegler, T. *J. Comput. Chem.* **2001**, *22*, 2001.

(17) Perdew, J. P.; Chevary, J. A.; Vosko, S. H.; Jackson, K. A.; Perderson, M. R.; Singh, D. J.; Fiolhais, C. *Phys. Rev. B* **1992**, *46*, 6671–6687. Erratum: Perdew, J. P.; Chevary, J. A.; Vosko, S. H.; Jackson, K. A.; Perderson, M. R.; Singh, D. J.; Fiolhais, C. *Phys. Rev. B* **1993**, *48*, 4978.

(18) Becke, A. D. *Phys. Rev.* **1988**, *A38*, 3098. Perdew, J. P. *Phys. Rev.* **1986**, *B33*, 8822. Erratum: Perdew, J. P. *Phys. Rev.* **1986**, *B34*, 7406.

(19) Becke, A. D. *Phys. Rev.* **1988**, *A38*, 3098.

(20) Perdew, N. J. P.; Burke, K.; Ernzerhof, M. *Phys. Rev. Lett.* **1996**, *77*, 3865–3868. Perdew, N. J. P.; Burke, K.; Ernzerhof, M. *Phys. Rev. Lett.* **1997**, *78*, 1396.

(21) Stephens, J.; Devlin, F. J.; Chabalowski, C. F.; Frisch, M. J. *J. Phys. Chem.* **1994**, *98*, 11623–11627.

(22) Reiher, M.; Salomon, O.; Hess, B. A. *Theor. Chem. Acc.* **2001**, *107*, 48.

(23) Bart, S. C.; Chlopek, K.; Bill, E.; Bouwkamp, M. W.; Lobkovsky, E.; Neese, F.; Wieghardt, K.; Chirik, P. J. *J. Am. Chem. Soc.* **2006**, *128*, 13901–13912.

(24) Selected studies comparing the performance of different functionals vis-à-vis transition metal spin state energetics: (a) Swart, M.; Groenhof, A. R.; Ehlers, A. W.; Lammertsma, K. *J. Phys. Chem. A* **2004**, *108*, 5479–5483. (b) Swart, M.; Ehlers, A. W.; Lammertsma, K. *Mol. Phys.* **2004**, *102*, 2467–2474. (c) Deeth, R. J.; Fey, N. *J. Comput. Chem.* **2004**, *25*, 1840–1848. (d) Groenhof, A. R.; Swart, M.; Ehlers, A. W.; Lammertsma, K. *J. Phys. Chem. A* **2005**, *109*, 3411–3417. (e) Daku, L. M. L.; Vargas, A.; Hauser, A.; Fouqueau, A.; Casida, M. E. *ChemPhysChem* **2005**, *6*, 1393–1410. (f) Ganzenmuller, G.; Berkaine, N.; Fouqueau, A.; Casida, M. E.; Reiher, M. *J. Chem. Phys.* **2005**, *122*, 234321. (g) De Angelis, F.; Jin, N.; Car, R.; Groves, J. T. *Inorg. Chem.* **2006**, *45*, 4268–4276. (h) Vargas, A.; Zerara, M.; Krausz, E.; Hauser, A.; Daku, L. M. L. *J. Chem. Theory Comput.* **2006**, *2*, 1342–1359. (i) Rong, C. Y.; Lian, S. X.; Yin, D. L.; Shen, B.; Zhong, A. G.; Bartolotti, L.; Liu, S. B. *J. Chem. Phys.* **2006**, *125*, 174102. (j) Strickland, N.; Harvey, J. N. *J. Phys. Chem. B* **2007**, *111*, 841–852. (k) Conradie, J.; Ghosh, A. *J. Phys. Chem. B* **2007**, *111*, 12621–12624.

(25) It should be noted that the ancillary ligand also plays a key role in tuning the energies of these MOs, and, with sufficiently weak-field supporting ligands, the ground-state may indeed turn out to be high-spin, as we predicted for an Fe^{III}(Tp)(NMe) complex (Tp = hydrotris(pyrazolyl)borate).[8]

CT800118C